



UNIVERSITI PUTRA MALAYSIA

***STRUCTURAL, MAGNETIC, ELECTRICAL AND MAGNETOTRANSPORT
PROPERTIES OF $(La,Pr)_{1-x}(Sr,Ba)_xMnO_3$ BULK, SINGLE AND BI-
LAYER THIN FILMS***

ALBERT GAN HAN MING

FS 2014 62



**STRUCTURAL, MAGNETIC, ELECTRICAL AND MAGNETOTRANSPORT
PROPERTIES OF $(La,Pr)_{1-x}(Sr,Ba)_xMnO_3$ BULK, SINGLE AND BI-LAYER
THIN FILMS**

ALBERT GAN HAN MING

**MASTER OF SCIENCE
UNIVERSITI PUTRA MALAYSIA**

2014



**STRUCTURAL, MAGNETIC, ELECTRICAL AND MAGNETOTRANSPORT
PROPERTIES OF $(La,Pr)_{1-x}(Sr,Ba)_xMnO_3$ BULK, SINGLE AND BI-LAYER
THIN FILMS**

ALBERT GAN HAN MING



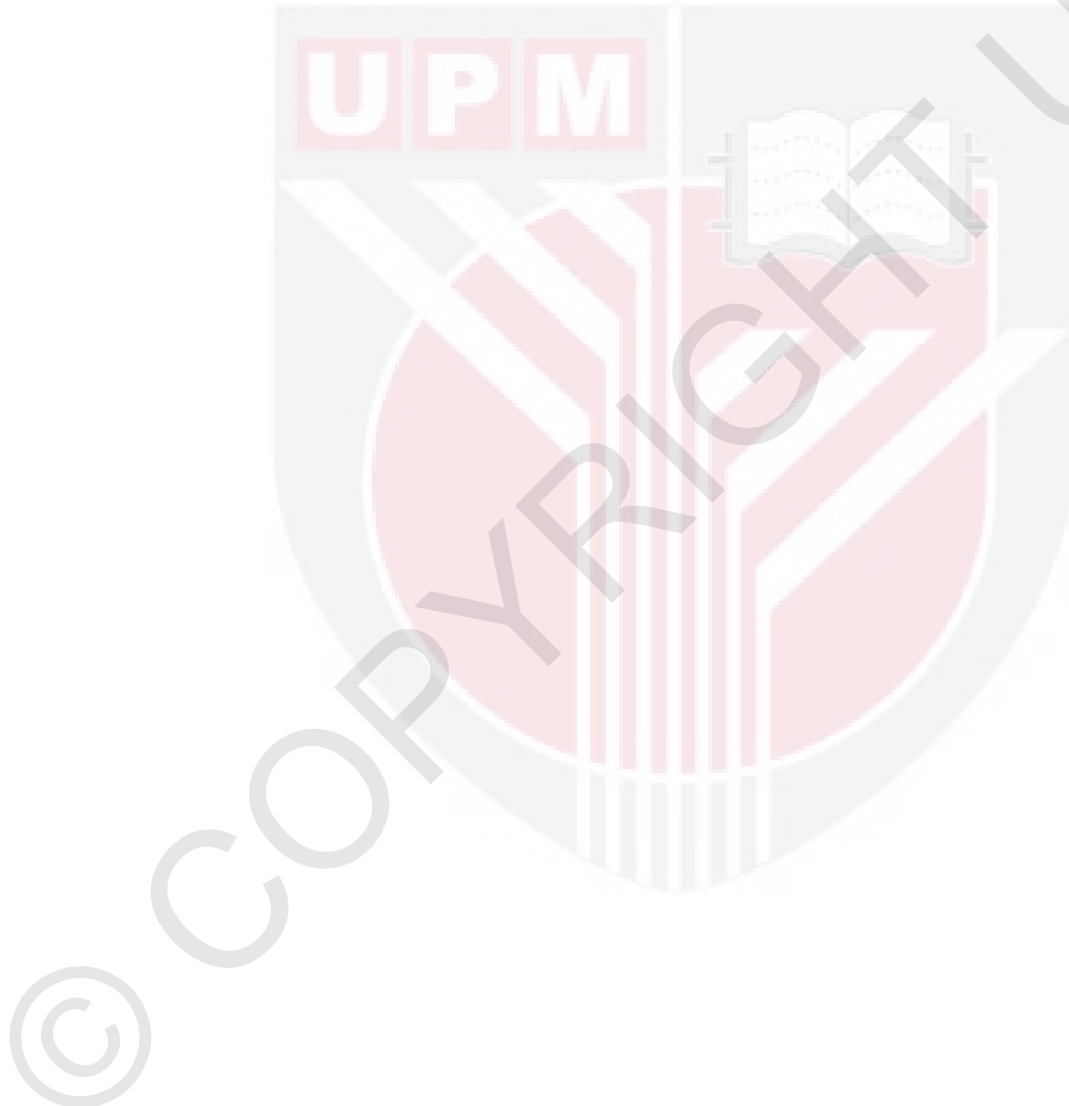
**Thesis Submitted to the School of Graduate Studies, Universiti Putra Malaysia, in
Fulfillment of the Requirements for the Degree of Master of Science**

September 2014

COPYRIGHT

All material contained within the thesis, including without limitation text, logos, icons, photographs and all other artwork, is copyright material of Universiti Putra Malaysia unless otherwise stated. Use may be made of any material contained within the thesis for non-commercial purposes from the copyright holder. Commercial use of material may only be made with the express, prior, written permission of Universiti Putra Malaysia.

Copyright © Universiti Putra Malaysia



Abstract of thesis presented to the Senate of Universiti Putra Malaysia in fulfillment of
the requirement for the degree of Master of Science

**STRUCTURAL, MAGNETIC, ELECTRICAL AND MAGNETOTRANSPORT
PROPERTIES OF $(La,Pr)_{1-x}(Sr,Ba)_xMnO_3$ BULK, SINGLE AND BI-LAYER
THIN FILMS**

By

ALBERT GAN HAN MING

September 2014

Chair: Lim Kean Pah, PhD

Faculty: Science

Colossal magnetoresistance (CMR) compound which exhibit large magnetoresistance value associated with its ferromagnetic-paramagnetic phase transition gain interest from researchers since 1950s. Large drop in resistivity in CMR material at very low magnetic field (0-0.1T) at low temperature (80K) gained further attentions from researchers. This low field magnetoresistance effect can be altered by grain size distribution. Fabrication and characterization of CMR thin film have been done in recent years to study the possibility in various application. Magnetic properties of thin film can be altered by introducing a pinning layer for bilayer film. Very limited report of coupling and stacking sequence of two CMR layer can be found. In this work, several investigation have been done. Effect of various average cation size of rare earth element and alkaline earth element at A-site towards physical properties in $(La,Pr)_{0.67}(Sr,Ba)_{0.33}MnO_3$ system have been studied. $La_{0.67}Sr_{0.33}MnO_3$ (LSMO), $Pr_{0.67}Sr_{0.33}MnO_3$ (PSMO), $La_{0.67}Ba_{0.33}MnO_3$ (LBMO), and $Pr_{0.67}Ba_{0.33}MnO_3$ (PBMO) were synthesized by conventional solid state reaction route. Sub-micron grains were obtained for the bulk samples. Transformation from hexagonal to orthorhombic crystal structure was observed when La^{3+} was replaced by Pr^{3+} . However, replacement of Sr^{2+} by Ba^{2+} in the compound only caused different microstructure formation. The difference in electrical, structural and magnetic properties in comparison to bulk samples are due to the difference in average cation size in A-site. T_p observed are >300 K for LSMO, 286 K for PSMO, 256 K for LBMO while PBMO shows T_p at 182 K and 150 K. Two T_p values in PBMO are due to the existing of core shell effect contributed by large difference in ionic size between rare earth and alkaline earth element. T_c observed for PSMO and PBMO are at 301 K and 184 K respectively. However, T_c of LSMO and LBMO were higher than 320 K similar as reported by other researchers. LSMO and PSMO were deposited on corning glass, MgO (100) and fused silica substrate by pulsed laser deposition technique (PLD). Grains obtained are in nano size and agglomerate in "island" like formation. Nano size cracks was observed due to difference in coefficient of thermal expansion between

sample and substrate. Crystal structure retain upon converted into thin film of thickness ~2 μm . Lattice strain induced from the lattice mismatch between sample and substrate affected Mn-O-Mn octahedral bond angle and bond distance, affected metal-insulator transition temperature in each system. Weak ferromagnetic behavior below T_c observed in PSMO-F can be due to the extremely high value of lattice strain induced. Bilayer thin film was synthesize by coupling LSMO and PSMO in different stacking sequences on top of corning glass, MgO (100) and fused silica. Larger grain size in bilayer film is due to the greater diffusion at second deposition. Lattice strain observed in bilayer system is dependent on the stacking sequence of crystal structure of individual film. The observed T_p of the top layer does not change much but curie temperature of top layer seemingly mimic to buffer layer due to magnetic pinning effect. Enhancement of magnetoresistance in bilayer film might due to the increase of disorder in bilayer system. $\text{Pr}_{0.67}\text{Sr}_{0.33}\text{MnO}_3$ with $\text{La}_{0.67}\text{Sr}_{0.33}\text{MnO}_3$ as buffer layer, deposited on MgO (100) showed highest LFMR value which is -14.4% at 80 K and 0.1 T whereas the LFMR value at room temperature (300K) is -0.9%. CMR material can be used for low/high field magnetic field sensing device, land mine detector (Roul *et al.*, 2001), as well as automotive sensors (NXP Semiconductors, 2006)

Abstrak tesis yang dikemukakan kepada Senat Universiti Putra Malaysia Sebagai memenuhi keperluan untuk ijazah Master Sains

**SIFAT-SIFAT STRUKTUR, MAGNET, ELEKTRIK DAN PENGANGKUTAN
MAGNETO UNTUK $(La,Pr)_{1-x}(Sr,Ba)_xMnO_3$ DALAM BENTUK PUKAL, FILEM
NIPIS DAN DWI LAPISAN**

Oleh

ALBERT GAN HAN MING

September 2014

Pengerusi: Lim Kean Pah, PhD

Fakulti: Sains

Bahan dengan magnetorintangan yang besar telah menarik perhatian penyelidik-penyalidik sejak tahun 1950 terutamanya keupayaan bahan tersebut dalam pertukaran sifat magnet daripada feromagnet kepada paramagnet. Pada suhu yang rendah (80K), rintangan bahan tersebut boleh mengurang dalam kadar yang besar hanya dengan aplikasi medan magnet yang rendah (0-0.1T). Sifat magnetorintangan pada suhu yang rendah ini boleh dipengaruhi oleh perubahan saiz purata butiran. Pembuatan dan pencirian filem nipis yang diperbuat daripada bahan magnetorintangan tersebut telah dijalankan oleh penyelidik-penyalidik untuk mengkaji penggunaanya dalam kehidupan kita. Sifat magnet dalam filem nipis boleh diubahsuai dengan memendapkan filem nipis ke atas lapisan filem nipis yang lain. Walaubagaimanapun laporan mengenai gandingan dan turutan dua filem yang berlainan dalam pembuatan dwi lapisan filem nipis adalah jarang. Dalam pengkajian ini, beberapa siasatan telah dibuat. Kesan terhadap sifat fizik dalam sistem $(La,Pr)_{0.67}(Sr,Ba)_{0.33}MnO_3$ dengan penggunaan saiz kation yang berlainan di bahagian A telah dikaji. $La_{0.67}Sr_{0.33}MnO_3$ (LSMO), $Pr_{0.67}Sr_{0.33}MnO_3$ (PSMO), $La_{0.67}Ba_{0.33}MnO_3$ (LBMO), dan $Pr_{0.67}Ba_{0.33}MnO_3$ (PBMO) diperbuat dengan kaedah tindak balas keadaan pepejal konvensional dan saiz bijiran dalam sub-mikron telah diperolehi. Sistem hablur mengalami transformasi dari heksagon kepada otorombik apabila La^{3+} diganti dengan Pr^{3+} . Tetapi, penggantian Sr^{2+} dengan Ba^{2+} hanya mengakibatkan mikrostruktur yang berlainan. Sifat elektrik, struktur dan magnet yang berlainan dalam sempel adalah disebabkan oleh perbezaan purata saiz kation yang berlainan di bahagian A. T_p yang diperhatikan adalah $>300K$ untuk LSMO, 286K untuk PSMO, 256K untuk LBMO manakala PBMO menunjukkan dua T_p di 182K dan 150K masing masing. Dua nilai T_p yang ditunjuk oleh PBMO adalah disebabkan oleh sifat shell dan teras yang berlainan. Ini adalah kerana perbezaan saiz ion yang besar antara unsur nadir bumi dan unsur alkali bumi. PSMO dan PBMO menunjukkan T_c pada suhu 301K dan 184K manakala nilai T_c yang ditunjukkan oleh PSMO dan PBMO adalah

lebih tinggi daripada suhu 320K. LSMO dan PSMO telah ditukar menjadi filem nipis berlapis tunggal dan dwi lapisan dengan teknik mendapan dedenyut laser (PLD) ke atas kaca corning, MgO(100) dan silika lakur. Bijiran yang didapati adalah dalam saiz nano dan menggumpal antara satu sama lain. Retakan dalam saiz nano didapati dalam filem nipis yang disebabkan oleh pengembangan terma yang berlainan antara sampel filem dan substrat. Sistem hablur tetap sama walaupun sempel dalam bentul filem nipis yang ketebalannya $\sim 2\mu\text{m}$. Regangan kekisi diakibatkan daripada ketidakseragaman kekisi antara filem dan substrat mempengaruhi sudut dan jarak antara Mn-O-Mn yang berbentuk lapan dan seterusnya menpengaruhi suhu transformasi logam-penebat dalam sistem-sistem. Sifat feromagnetik yang lemah pada suhu di bawah T_c di sempel PSMO-F adalah disebabkan oleh regangan kekisi yang lebih tinggi. Filem dwi lapisan telah pun dihasilkan dengan LSMO dan PSMo dalam turutan mendapan yang berlainan di kaca corning, MgO(100) dan silika lakur. Saiz bijiran yang lebih besar dalam filem dwi lapisan adalah disebabkan oleh resapan yang lebih besar antara bijiran pada masa pemendapan yang kedua. Regangan kekisi yang didapati dalam sistem dwi lapisan adalah bergantung kepada turutan dalam mendapan filem-filem yang mempunyai sistem hablur yang berlainan. T_p untuk filem pada lapisan atas tidak banyak berubah manakala suhu curie dari filem lapisan atas seolah-olah meniru daripada filem di lapisan bawah. Ini adalah disebabkan oleh kesan penyematan magnetik. Sifat magnetorintangan dalam dwi lapisan yang lebih kuat mungkin juga disebabkan oleh kecelaruan yang lebih tinggi dalam sistem. $\text{Pr}_{0.67}\text{Sr}_{0.33}\text{MnO}_3$ yang mendap atas $\text{La}_{0.67}\text{Sr}_{0.33}\text{MnO}_3$ di substrat MgO(100) telah menunjukkan magnetorintangan yang paling besar iaitu -14.4% pada suhu 80K dengan medan magnet 0.1T. Bahan yang mempersembahkan magnetorintangan boleh digunakan sebagai sensor magnet, pengesan ranjau letupan darat, dan juga sensor kereta.

ACKNOWLEDGEMENTS

First of all I would like to express my gratitude to my supervisor, Assoc. Prof. Dr. Lim Kean Pah for his patience, guidance, advice as well as discussions throughout these years. I also like to thank my co-supervisor Prof. Dr. Zainal Abidin Talib, Prof. Dr. Abdul Halim Shaari and Assoc. Prof. Dr Chen Soo Kien for their help in doing research and I come to know about so many new things. I am really thankful to them. My sincere thanks to all other lecturers as well as staff in the Department of Physics, Faculty of Science who gave their help, contributed directly or indirectly in my research. My special thanks to Wong Jen Kuen, Ng Siau Wei, Chin Hui Wei, Cheong Kuen Hou, Tan Kwee Yong, Tan Kim Lee and other lab mates who help and guided me in my research. My greatest appreciation to my family members especially my parents, brother, sister and my relatives for their support and understanding throughout the years.





This thesis was submitted to the Senate of Universiti Putra Malaysia and has been accepted as fulfilment of the requirement for the degree of Master of Science. The members of the Supervisory Committee were as follows:

Lim Kean Pah, PhD

Associate Professor

Faculty of Science

Universiti Putra Malaysia

(Chairman)

Zainal Abidin Talib, PhD

Professor

Faculty of Science

Universiti Putra Malaysia

(Member)

Chen Soo Kien, PhD

Associate Professor

Faculty of Science

Universiti Putra Malaysia

(Member)

BUJANG BIN KIM HUAT, PhD

Professor and Dean

School of Graduate Studies

Universiti Putra Malaysia

Date:

Declaration By Graduate Student

I hereby confirm that:

- this thesis is my original work;
- quotations, illustrations and citations have been duly referenced;
- this thesis has not been submitted previously or concurrently for any other degree at any other institutions;
- intellectual property from the thesis and copyright of thesis are fully-owned by Universiti Putra Malaysia, as according to the Universiti Putra Malaysia (Research) Rules 2012;
- written permission must be obtained from supervisor and the office of Deputy Vice-chancellor (Research and Innovation) before thesis is published (in the form of written, printed or in electronic form) including books, journals, modules, proceedings, popular writings, seminar papers, manuscripts, posters, reports, lecture notes, learning modules or any other materials as stated in the Universiti Putra Malaysia (Research) Rules 2012;
- there is no plagiarism or data falsification/fabrication in the thesis, and scholarly integrity is upheld as according to the Universiti Putra Malaysia (Graduate Studies) Rules 2003 (Revision 2012-2013) and the Universiti Putra Malaysia (Research) Rules 2012. The thesis has undergone plagiarism detection software.

Signature: _____

Date: _____

Name and Matric No.: _____

Declaration by Members of Supervisory Committee

This is to confirm that:

- the research conducted and the writing of this thesis was under our supervision;
- supervision responsibilities as stated in the Universiti Putra Malaysia (Graduate Studies) Rules 2003 (Revision 2012-2013) are adhered to.

Signature: _____

Name of chairman of Supervisory Committee: _____

Signature: _____

Name of Member of Supervisory Committee: _____

Signature: _____

Name of Member of Supervisory Committee: _____

TABLE OF CONTENTS

	Page
ABSTRACT	i
ABSTRACT	iv
ACKNOWLEDGEMENT	vii
APPROVAL	viii
DECLARATION	ix
LIST OF TABLES	xvi
LIST OF FIGURES	xvii
LIST OF ABBREVIATIONS	xxv
CHAPTER	
1	
INTRODUCTION	1
1.1 Magnetoresistance Material	1
1.2 Problem Statement	2
1.3 Objective	3
1.4 Thesis Structure	3
2	
LITERATURE REVIEW	4
2.1 Historical Background	4
2.2 Influence of Doping in Structural Properties	4
2.3 Influence of Synthesis Method on Microstructure Properties	7
2.4 Influence of Doping in Electrical Properties	13
2.5 Influence of Lattice Strain in Electrical Properties	17
2.6 Influence of Doping in Magnetotransport Properties	19
2.7 Influence of Lattice Strain in Magnetotransport Properties	22
2.8 Magnetoresistance and Magnetic Behavior in Manganite	25
2.9 Influence of Stacking in Manganite Film	29
2.10 Influence of Double Exchange Effect and Jahn-Teller Effect	31
3	
THEORY	32
3.1 Magnetoresistance	32
3.2 Type of Magnetoresistance	33
3.2.1 Ordinary Magnetoresistance (OMR)	33
3.2.2 Anisotropic Magnetoresistance (AMR)	33
3.2.3 Giant Magnetoresistance (GMR)	33
3.2.4 Tunneling Magnetoresistance (TMR)	34
3.2.5 Colossal Magnetoresistance (CMR)	34
3.3 Perovskite structure	35
3.4 Low field magnetoresistance Effect	35
3.5 Double Exchange mechanism	35

3.6 Jahn-Teller Effect	36
3.7 Pulsed Laser Deposition	37
3.8 Growth Mode In PLD	38
3.8.1. Volmer-Weber Growth Mode (Island Growth)	39
3.8.2. Frank-Van der Merwe (Layer By Layer Growth)	39
3.8.3. Stranski-Krastanov (Mixed Growth)	39
3.8.4. Step-flow growth mode	40
3.8.5. Step bunching growth mode	40
3.8.6. Spiral-island growth mode	40
3.8.7. Epitaxial growth mode	40
3.9 Substrate Properties	41
3.10 Magnetism	41
3.10.1 Ferromagnetic Behavior	41
3.10.2 Paramagnetic Behavior	41
3.11 Lattice Strain Effect	42
4 MATERIALS AND METHODS	44
4.1 Sample preparation for bulk samples by solid state reaction	44
4.1.1 Mixing and Milling Process	45
4.1.2 Calcination Process	46
4.1.3 Grinding and Sieving Process	46
4.1.4 Pelletizing and Sintering Process	46
4.1.5 Pulsed Laser Deposition Process	47
4.2 Sample Characterization	49
4.2.1 X-ray Diffraction	49
4.2.2 Scherrer Equation	50
4.2.3 Gonio Scan	50
4.2.4 Two Theta Scan	51
4.3 Microstructure Observation (Scanning Electron Microscope, SEM and Field Emission Scanning Electron Microscope, FESEM)	51
4.4 Magnetic Properties Characterization By Vibrating Sample Magnetometer (VSM, Lakeshore 7400)	52
4.5 Electrical Properties By Lake Shore Hall Effect Measurement System 7604	52
4.6 Thickness measurement by Stylus Profiler XP2000	53
4.7 Magnetoresistance Measurement	54
4.8 AC Susceptibility Measuring System (CryoBind T)	54
5 RESULTS AND DISCUSSIONS	56
5.1 Bulk System	57
5.1.1 X-ray Diffraction (XRD) Analysis	57
5.1.2 Microstructure Analysis of Bulk Samples	60
5.1.3 AC Susceptibility	61

5.1.4 Resistivity and Phase Transition Temperature	62
5.1.5 Colossal Magnetoresistance Effect	63
5.2 LSMO Single Layer Thin Film System	67
5.2.1 XRD analysis of LSMO Thin Film	67
5.2.2 Microstructure Analysis of LSMO Thin Film	70
5.2.3 AC Susceptibility	71
5.2.4 Resistivity and Phase Transition Temperature	71
5.2.5 Colossal Magnetoresistance Effect	72
5.3 PSMO Single Layer Thin Film System	77
5.3.1 XRD Analysis of PSMO Thin Film	77
5.3.2 Microstructure Analysis of PSMO thin film	80
5.3.3 AC Susceptibility	81
5.3.4 Resistivity and Phase Transition Temperature, T_p	82
5.3.5 Colossal Magnetoresistance Effect	83
5.4 LS/PS Bilayer Thin Film System	87
5.4.1 XRD Analysis of LS/PS Thin Film System	87
5.4.2 Microstructure Analysis of LS/PS Thin Film	89
5.4.3 AC susceptibility	90
5.4.4 Resistivity and Phase Transition Temperature, T_p	90
5.4.5 Colossal Magnetoresistance Effect	91
5.5 PS/LS Bilayer Thin Film System	94
5.5.1 XRD Analysis of PS/LS Thin Film System	94
5.5.2 Microstructure Analysis of PS/LS Thin Film	96
5.5.3 AC Susceptibility	97
5.5.4 Resistivity and Phase Transition Temperature, T_p	98
5.5.5 Colossal Magnetoresistance Effect	99
6 CONCLUSION	103
6.1 Conclusion	103
6.2 Suggestion of Future Work	104
REFERENCES	105
APPENDICES	110
BIODATA OF STUDENT	118
LIST OF PUBLICATIONS & CONFERENCES ATTENDED	119

LIST OF TABLES

Table	Page
2.1 T _N , T _C , and M _S mean the Neel temperature, the Curie temperature, and the saturated magnetization, respectively reported for La _{1-x} Sr _x MnO ₃	5
2.2 Comparison of Researchers' Work for Quick Reference I	7
2.3 Comparison of Researchers' Work for Quick Reference II	13
2.4 Details of LCMO/STO(200), LCMO/STO(50), and	17
2.5 Electrical and structural parameters of LCMO films	18
2.6 Comparison of Researchers' Work for Quick Reference III	19
2.7 Comparison of Researchers' Work for Quick Reference IV	22
2.8 Comparison of Researchers' Work for Quick Reference V	25
2.9 Comparison of Researchers' Work for Quick Reference VI	27
2.10 Comparison of Researchers' Work for Quick Reference VII	30
5.1 Abbreviation and description of Bulk samples	56
5.2 Abbreviation and description of single layer thin film samples	56
5.3 Abbreviation and description of bi-layer thin film samples	57
5.4 Rietveld Refinement crystallography data of (La,Pr) _{0.67} (Sr,Ba) _{0.33} MnO ₃ system	59
5.5 Rietveld Refinement crystallography data of (La,Pr) _{0.67} (Sr,Ba) _{0.33} MnO ₃ system	69
5.6 Rietveld Refinement Crystallography Data for PSMO Bulk and Thin Film System	79
5.7 Rietveld Refinement Crystallography Data for LSMO Single Layer Thin Film and LS/PS Bilayer Thin Film	88
5.8 Rietveld Refinement Crystallography Data for PSMO Single Layer Thin Film and PS/LS Bilayer Thin Film.	96

LIST OF FIGURES

Figure	Page
2.1 XRD patterns of (100) LBMO films on (a) STO, (b) NGO, (c) LAO, and (d) MgO. Dashed line indicates the peak position of the bulk LBMO. Inset: schematic pictures to show the type of the in-plane stress expected from lattice mismatch	6
2.2 Scanning electron micrographs of $\text{Pr}_{2/3}\text{Ba}_{1/3}\text{MnO}_3$ and $\text{La}_{2/3}\text{Ca}_{1/3}\text{MnO}_3$	7
2.3 SEM micrograph of $\text{La}_{0.8}\text{Sr}_{0.3}\text{MnO}_3$ milled for (a) 1 hour, (b) 48 hours, (c) 72 hours	9
2.4 SEM photograph of $\text{La}_{0.7}\text{Sr}_{0.3}\text{MnO}_3$ sintered at 1200°C for 4h	9
2.5 SEM micrographs of $\text{La}_{0.86}\text{K}_{0.3}\text{MnO}_3$ sintered at : (a) 750°C , (b) 800°C , (c) 900°C , (d) 1000°C	10
2.6 STM image for $\text{La}_{0.67}\text{Ca}_{0.33}\text{MnO}_3$ thin film (a) as grown, (b) annealed	11
2.7 Topography STM image of (a)LCMO/STO (200nm), (b) LCMO/STO (50nm) and (c)LCMO/NGO (50nm)	11
2.8 STM shows different surface topography of 500 Å LSMO films grown on different (a)NGO (b) LSAT and (c) LAO substrate for scan size of $1.0 \times 1.0 \mu\text{m}^2$	12
2.9 Electronic phase diagram of $\text{La}_{1-x}\text{Sr}_x\text{MnO}_3$	14
2.10 Electronic phase diagram of $\text{Pr}_{1-x}\text{Sr}_x\text{MnO}_3$	15
2.11 Resistivity-temperature variation of $\text{Pr}_{2/3}\text{Ba}_{1/3}\text{MnO}_3$ and $\text{La}_{2/3}\text{Ca}_{1/3}\text{MnO}_3$	16
2.12 Temperature dependence of the resistivity for $\text{La}_{0.8}\text{Sr}_{0.2}\text{MnO}_3$	16
2.13 Resistivity versus temperature for 80nm LBMO films grown on STO and LAO substrates	18
2.14 Temperature dependence of susceptibility registered for $\text{Pr}_{0.7}\text{Ca}_{0.20}\text{Sr}_{0.10}\text{MnO}_3$ (a), $\text{Pr}_{0.7}\text{Ca}_{0.25}\text{Sr}_{0.05}\text{MnO}_3$ (b), and $\text{Pr}_{0.7}\text{Ca}_{0.3}\text{MnO}_3$ (c). In (d) the corresponding magnetization curves registered in 1.4T after a zero field cool process	20
2.15 Plots of AC susceptibility versus temperature (K) of Pr-based samples	21
2.16 Plot of real part susceptibility versus temperature for $\text{Pr}_{2/3}\text{Ba}_{1/3}\text{MnO}_3$ and imaginary susceptibility $\text{La}_{2/3}\text{Ca}_{1/3}\text{MnO}_3$ (a) and $\text{Pr}_{2/3}\text{Ba}_{1/3}\text{MnO}_3$ and $\text{La}_{2/3}\text{Ca}_{1/3}\text{MnO}_3$ (b)	21
2.17 Magnetization versus temperature graphs of the LBMO films grown on LAO substrate under 0.5T	23

2.18	Magnetization versus temperature graphs of the LBMO films grown on STO substrate under 0.5T	23
2.19	T_c of LBMO thin film as a function of thickness	24
2.20	MR variation with applied magnetic field of $\text{Pr}_{2/3}\text{Ba}_{1/3}\text{MnO}_3$ and $\text{La}_{2/3}\text{Ca}_{1/3}\text{MnO}_3$ at 77 K	26
2.21	Resistivity-temperature variation with and without magnetic field and MR behaviour of (a) $\text{Pr}_{2/3}\text{Ba}_{1/3}\text{MnO}_3$ and (b) $\text{La}_{2/3}\text{Ca}_{1/3}\text{MnO}_3$	27
2.22	Plot of M (emu/g) vs. H (Gauss) of Pr-based samples	28
2.23	Left: Temperature dependence of resistance for LSMO, LCMO and Bilayer films without (solid symbols) and with (open symbols) an applied magnetic field of 5 T. Arrows show the temperatures for T_p . Right: (a) Temperature dependence of Field cooled (solid symbols) and zero field cooled (open symbols) magnetization for LSMO (1) and LCMO (2) and Bilayer (3) films. Arrows indicate the temperature for the magnetic transition. Dashed line was obtained by a simple addition of the field cooled curves (1) and (2), (b) Temperature dependence of susceptibility for LSMO (1), LCMO (2) and Bilayer (3) films	29
2.24	(Color online) Temperature dependence of the magnetoresistivity MR perpendicular and MR parallel in a field of 6.8 kG for two different H-J configurations.	30
3.1	Resistance versus applied magnetic field for a magnetoresistive material	32
3.2	Perovskite structure	35
3.3	Schematic diagram of double exchange mechanism	36
3.4	Splitting of 3d levels into lower t_{2g} and higher e_g levels in Manganese	37
3.5	Schematic draw of the elementary processes during nucleation	39
3.6	Schematic draw of different growth modes of substrate-film	40
3.7	Schematic draw of ferromagnetism with or without magnetic field within grain boundary	41
3.8	Schematic draw of paramagnetism with or without magnetic field within grain boundary	42
3.9	Schematic draw of lattice misfit of film and substrate in compression and elongation	43
4.1	Solid State Reaction Route for Bulk Sample Preparation	44
4.2	Wet Milling	45
4.3	Temperature Versus Time Graph for Calcination Process	46
4.4	Temperature Versus Time Graph for Sintering Process	47
4.5	Schematic Draw for Pulsed Laser Deposition Set-up	48
4.6	Schematic Draw for X-ray Diffraction Effect	49
4.7	Schematic Draw for Gonio Scan Technique	50

4.8	Schematic Draw for Two Theta Scan Technique	51
4.9	Schematic Draw of Four Point Probe Measurement Method	53
4.10	Schematic Draw of Measurement by Stylus Profiler	53
4.11	AC Susceptibility System	55
5.1	X-ray Diffraction Pattern of $(La,Pr)_{0.67}(Sr,Ba)_{0.33}MnO_3$ system at room temperature	58
5.2	X-ray Diffraction Pattern at Peak of $(La,Pr)_{0.67}(Sr,Ba)_{0.33}MnO_3$ system	59
5.3	SEM Micrograph of $(La,Pr)_{0.67}(Sr,Ba)_{0.33}MnO_3$ samples at 3kX Magnification	60
5.4	Normalized Ac Susceptibility Versus Temperature Graph for $(La,Pr)_{0.67}(Sr,Ba)_{0.33}MnO_3$ System	61
5.5	Resistivity Versus Temperature Graph of $(La,Pr)_{0.67}(Sr,Ba)_{0.33}MnO_3$ System	63
5.6	MR% Versus Applied Field at Room Temperature for $(La,Pr)_{0.67}(Sr,Ba)_{0.33}MnO_3$ System	65
5.7	MR% Versus Temperature Graph for $(La,Pr)_{0.67}(Sr,Ba)_{0.33}MnO_3$ System	66
5.8	Magnetization as a Function of Magnetic Field Strength for $(La,Pr)_{0.67}(Sr,Ba)_{0.33}MnO_3$ System	67
5.9	X-ray Diffraction Pattern of $La_{0.67}Sr_{0.33}MnO_3$ Thin Film System at Room Temperature	68
5.10	X-ray Diffraction Pattern at Peak of $La_{0.67}Sr_{0.33}MnO_3$ Thin Film System	69
5.11	SEM and FESEM Micrograph of LSMO Bulk and LSMO Thin Film System at 3kX and 200kX magnification respectively. (Inset: 50kX)	70
5.12	Normalized Ac Susceptibility of LSMO Bulk and LSMO Thin Film System	71
5.13	Resistivity Versus Temperature Graph for LSMO Bulk and LSMO Thin Film System	72
5.14	MR% Versus Applied Magnetic Field for LSMO Thin Film System	75
5.15	MR% Versus Temperature Graph for LSMO Bulk and LSMO Thin Film System	76
5.16	Magnetization as a Function of Magnetic Field Strength for LSMO Bulk and LSMO Thin Film System	77
5.17	X-ray Diffraction Pattern of PSMO Bulk and PSMO Thin Film System at Room Temperature	78
5.18	X-ray Diffraction Pattern at Peak of $Pr_{0.67}Sr_{0.33}MnO_3$ Bulk and Thin Film System	79
5.19	SEM and FESEM Micrograph of PSMO Bulk and Thin Film System at 3kX and 50kX magnification respectively. (Inset: 200kX)	80

5.20	Normalized Ac Susceptibility Versus Temperature Graph for PSMO Bulk and Thin Film System	81
5.21	Resistivity Versus Temperature Graph for PSMO Thin Film System	83
5.22	Resistivity Versus Temperature Graph for PSMO Bulk System	83
5.23	MR% Versus Applied Magnetic Field Strength for PSMO Thin Film System	85
5.24	MR% Versus Temperature Graph for PSMO Bulk and Thin Film System	86
5.25	Magnetization as a Function of Magnetic Field Strength for PSMO Bulk and Thin Film System	87
5.26	X-ray Diffraction Pattern of LSMO Bulk, LSMO Single Layer Thin Film, and LS/PS Bilayer Thin Film	88
5.27	FESEM Micrograph of LS/PS Bilayer Film at 10kX magnification and 30kX (inset) magnification respectively	89
5.28	Normalized Ac Susceptibility Versus Temperature Graph for LSMO Bulk, LSMO Single Layer Thin Film and LS/PS Bilayer Thin Film	90
5.29	Resistivity Versus Temperature Graph for LS/PS Bilayer Thin Film	91
5.30	MR% Versus Applied Magnetic Field Strength for LS/PS Bilayer Thin Film	93
5.31	MR% Versus Temperature Graph for LSMO Bulk, LSMO Single Layer Thin Film, LS/PS Bilayer Thin Film	94
5.32	X-ray Diffraction Pattern for PSMO Bulk, PSMO Single Layer Thin Film, and PS/LS Bialyer Thin Film	95
5.33	FESEM Micrograph of PS/LS Bilayer Thin Film at 5kX and 30kX(inset) magnification	97
5.34	Normalized Ac Susceptibility Versus Temperature Graph for PSMO Bulk, PSMO Single Layer Thin Film, PS/LS Bilayer Thin Film	98
5.35	Resistivity Versus Temperature Graph for PS/LS Bilayer Thin Film	99
5.36	MR% Versus Applied Magnetic Field Strength for PS/LS Bilayer Thin film	101
5.37	MR% Versus Temperature Graph for PSMO Bulk, PSMO Single Layer Thin Film, and PS/LS Bilayer Thin film	102

LIST OF ABBREVIATIONS

AE	Alkaline Earth Element
RE	Rare Earth Element
%MR	Percentage of Magnetoresistance
MR	Magnetoresistance
CMR	Colossal Magnetoresistance
LFMR	Low Field Magnetoresistance
SEM	Scanning Electron Microscope
FESEM	Field Emission Electron Microscope
XRD	X-ray Diffraction
Mn-O	Bond distance between Manganese Ion and Oxygen Ion.
Å	Angstrom
%	Percentage
K	Kelvin
T _c	Curie Temperature
T _p	Metal-Insulator Transition Temperature
ICSD	Inorganic Crystal Structure Database
SSMO	$\text{Sm}_{0.55}\text{Sr}_{0.45}\text{MnO}_3$
NDMO	$\text{Nd}_{0.55}\text{Sr}_{0.45}\text{MnO}_3$

CHAPTER 1

INTRODUCTION

1.1 Magnetoresistance Material

Several types of magnetoresistanc(MR) effect and these include Ordinary MR, Anisotropic MR, Giant MR, Tunneling MR and Colossal MR. All these MR effects were exhibited through different combinations of element where the resistivity droped with certain applied magnetic field strength. Colossal magnetoresistance (CMR) which was known to exist since 1950 gained interest from researchers due to its large magnetoresistance value associated with its ferromagnetic-paramagnetic phase transition. Apart from this, low field magnetoresistance effect where larger drop in resistivity in CMR material at very low magnetic field (0-0.1T) at low temperature gained further attentions because this magnetic field strength region is suitable for application in magnetic reading devices (Ramirez *et al.*, 1997). Most of the manganite compound followed the general formula $RE_{1-x}AE_xMnO_3$ where RE= trivalent element, AE=divalent element. The electric and magneto transport properties at temperatures lower than T_c/T_p are mainly contributed by double exchange mechanism. At low temperature, compound in ferromagnetic state have most of the electron spin arranged in the same direction. Electron from the 3d orbital of Mn^{3+} can easily hop to Mn^{4+} through oxygen atom thus creating the movement of electron in the structure. This double exchange (DE) mechanism can easily be affected by the alignment of the electron spin and thus applied magnetic field could smoothen the electron hopping process and lowering down the resistivity value. However, double exchange mechanism itself cannot describe the conducting phenomena in CMR compound. Above T_c , CMR compound turns into paramagnetic state where the electron spin fluctuated and disordered. DE mechanism is then weakened. Jahn-Teller theory was introduced to mention the conducting effect at above T_c with the coexistence of Hund's coupling effect. Electrons in the structure can hop when MnO_6 octahedral remove the degeneracy by displacing from its original position.

Thin film gained interest from researchers due to its potential application. Upon converting bulk manganite into thin film, several factors like type of substrate used, annealing temperature, synthesis technique (Fors *et al.*,2004; Fang *et al.*, 2011; Malisa and Ivanov, 2005), film thickness and etc have to be taken into consideration. These factors affect the physical properties like microstructure formation and thus electro/magneto transport properties. However, there are still a lot more investigation yet to be done on these manganite materials.

1.2 Problem Statement

Taran *et al.* (2006) prepared single layer and bilayer thin film of $\text{La}_{0.67}\text{Sr}_{0.33}\text{MnO}_3$ (SL1), $\text{La}_{0.67}\text{Ca}_{0.33}\text{MnO}_3$ (SL2) and $\text{La}_{0.67}\text{Sr}_{1.33}\text{MnO}_4$ (SL3) on SrTiO_3 (001) substrate by RF (radio frequency) magnetron sputtering technique. Large enhancement of magnetoresistance at 1.2T field from 8% (SL1) and 35% (SL2) to 12%(SL1/SL3) and 50%(SL2/SL3). T_p reported shifted towards lower temperature (370 K for SL1 and 295 K for SL1/SL3) due to the increase of disorder and strain effect in bilayer film. The same thing happen for SL2 and SL2/SL3 where T_p drops from 248 K to 225 K. This phenomena is due to strain induced from unequal structure as reported. SEM micrograph of single layer film system showed average grain size around ~ 100 nm. Increase of MR in bilayer system was due to the increase in disorder. Park *et al.* (2004) also fabricate bilayer $\text{La}_{0.8}\text{Sr}_{0.2}\text{MnO}_3/\text{La}_{0.8}\text{Ca}_{0.2}\text{MnO}_3$ by rf sputtering technique. T_p of LSMO and LCMO reported are about the same which is at 230 K but shifted to 280 K in bilayer form. Increased in T_c also reported in bilayer film as T_c of bilayer is about 280 K while T_c of LSMO and LCMO are found 260 K and 230 K respectively. Effect of lattice strain in $\text{La}_{0.8}\text{Sr}_{0.2}\text{MnO}_3/\text{La}_{0.8}\text{Ca}_{0.2}\text{MnO}_3$ bilayer grown on LaAlO_3 (001) was studied by Prokhorov *et al.* (2007). Lattice parameter of the top layer, $\text{La}_{0.8}\text{Sr}_{0.2}\text{MnO}_3$ is dependent on the buffer layer/substrate's c-axis as reported. T_p shifted to higher temperature where T_p is of single layer film $\text{La}_{0.8}\text{Sr}_{0.2}\text{MnO}_3$ and $\text{La}_{0.8}\text{Ca}_{0.2}\text{MnO}_3$ reported are very close at about 230 K while bilayer film is at 280 K. Changes in lattice parameter C for $\text{La}_{0.8}\text{Sr}_{0.2}\text{MnO}_3$ in bilayer improve magnetic and electronic properties. However, not much work and studies on the microstructure properties in bilayer film. Very few report can be found for coupling effect and stacking sequences effect of two type of manganite film. So, investigation in certain area is important such as:

1. The effect of average cation radius changed in $\text{RE}_{1-x}\text{AE}_x\text{MnO}_3$ by substitution of rare earth element or alkaline earth element in structural, electrical and magnetotransport properties.
2. The substrate effect towards structural, electrical and magnetotransport properties of CMR material upon converted into thin film.
3. The effect of thin film coupling by LSMO ($T_c > 300\text{K}$) and PSMO ($T_c < 300\text{K}$) towards structural, electrical and magnetotransport properties as well as influence brought by stacking sequences.

1.3 Objective

In bulk system, varied rare earth element ($\text{La}^{3+}, \text{Pr}^{3+}$) and alkaline element ($\text{Sr}^{2+}, \text{Ba}^{2+}$) in manganese compound were studied. All CMR compounds followed the general formula $\text{RE}_{0.67}\text{AE}_{0.33}\text{MnO}_3$ (RE: rare earth element; AE: alkaline earth element) to fix the ratio of $\text{Mn}^{3+}/\text{Mn}^{4+}$ so that comparison can be made. Single layer thin film was fabricated on various substrate to study the substrate effect. The bi-layer thin film coupling by $\text{La}_{0.67}\text{Sr}_{0.33}\text{MnO}_3$ which showed high phase transition temperature ($>300\text{K}$) and $\text{Pr}_{0.67}\text{Sr}_{0.33}\text{MnO}_3$ with low transition ($<300\text{K}$) were interested to study by varying the stacking sequence. In this work, the objective is:

1. To fabricate $\text{La}_{0.67}\text{Sr}_{0.33}\text{MnO}_3$, $\text{La}_{0.67}\text{Ba}_{0.33}\text{MnO}_3$, $\text{Pr}_{0.67}\text{Sr}_{0.33}\text{MnO}_3$, and $\text{Pr}_{0.67}\text{Ba}_{0.33}\text{MnO}_3$ bulk samples via solid state reaction method and characterize in structural, electrical, and magnetotransport properties.
2. To fabricate single layer thin film of $\text{La}_{0.67}\text{Sr}_{0.33}\text{MnO}_3$, $\text{La}_{0.67}\text{Ba}_{0.33}\text{MnO}_3$, $\text{Pr}_{0.67}\text{Sr}_{0.33}\text{MnO}_3$, and $\text{Pr}_{0.67}\text{Ba}_{0.33}\text{MnO}_3$ deposited on amorphous (corning glass and fused silica) and single crystal (MgO 100) substrate via pulsed laser deposition method and characterize in structural, electrical, and magnetotransport properties.
3. To fabricate bi-layer thin film of $\text{La}_{0.67}\text{Sr}_{0.33}\text{MnO}_3$ and $\text{Pr}_{0.67}\text{Sr}_{0.33}\text{MnO}_3$ by varied the stacking sequence on amorphous (corning glass and fused silica) and single crystal (MgO 100) substrate via pulsed laser deposition method and characterize in structural, electrical, and magnetotransport properties.

1.4 Thesis Structure

Some literature review and simple theory were showed in Chapters 2 and 3. Solid state sintering technique, pulsed laser deposition technique, the machine and skill used to characterize the structure, microstructure, magnetoresistance, electric and magnetotransport, are explained in Chapter 4 (methodology). Analysis of result and comparisons were showed in Chapter 5 (result and discussion). Last but not least, conclusion was made in chapter 6. References and Appendix were attached at the end of the thesis.

REFERENCES

- Anil Kumar, P. S., Joy, P. A., Date, S. K. (1998). Comparison of the Low Field Magnetic Behavior of $\text{Ln}_{0.7}\text{Ca}_{0.3}\text{MnO}_3$ ($\text{Ln} = \text{La}, \text{Pr}$). *Solid State Communications* 108 (2), 67- 70.
- Daoudi, K., Oueslati, M., Tsuchiya, T., Nakajima, T., Kawaguchi, K. (2010). Strain Effect on the Electrical and Magnetic Properties of $\text{La}_{0.7}\text{Ba}_{0.3}\text{MnO}_3$ Thin Films Grown by Metal Organic Deposition. *Journal of Superconductivity and Novel Magnetism* 23 , 1355-1358.
- Dey, P., Nath, T. K., Taraphder, A. (2007). Effect of Substrate-induced Strain on Transport and Magnetic Properties of Epitaxial $\text{La}_{0.66}\text{Sr}_{0.33}\text{MnO}_3$ Thin Films. *Applied Physics Letters* 91 (1) 012511 , 012511-012513.
- Du, Y., Zhang, X., Yu, D. Yan, H. (2006). Microstructure and Properties of $\text{La}_{0.7}\text{Sr}_{0.3}\text{MnO}_3$ Films Deposited on LaAlO_3 (100), (110) and (111) Substrates. *Journal of Rare Earths* 24 (5) , 560-563.
- Egilmez, M., Abdelhadi, M., Salman, Z., Chow, K. H., Jung, J. (2009). Enhancement of the Magnetotransport and Magnetoresistive Anisotropy in $\text{Sm}_{0.55}\text{Sr}_{0.45}\text{MnO}_3/\text{Nd}_{0.55}\text{Sr}_{0.45}\text{MnO}_3$ Bilayers. *Applied Physics Letters* 95 , 112505.
- Ellouze, M., Boujelben, W., Cheikhrouhou, A., Fuess, H., Madar, R. (2003). Structure, Ferromagnetism, and Magnetotransport Properties in the Barium-deficient $\text{Pr}_{0.7}\text{Ba}_{0.2}\&0.1\text{MnO}_3$. *Journal of Magnetism and Magnetic Materials* 257 , 319-326.
- Fang, S., Pang, Z., Wang, F., Lin, L., Han, S. (2011). Annealing Effect on Transport and Magnetic Properties of $\text{La}_{0.67}\text{Sr}_{0.33}\text{MnO}_3$ Thin Films Grown on Glass Substrate by RF Magnetron Sputtering. *Journal of Materials Science and Technology* 27(3), 223-226.
- Fors, R., Khartsev, S., Grishin, A., Pohl, Annika., Westin, Gunnar. (2004). Sol-gel Derived Versus Pulsed Laser Deposited Epitaxial $\text{La}_{0.67}\text{Ca}_{0.33}\text{MnO}_3$ Films: Structure, Transport and Effects of Post-Annealing. *Thin Solid Films* 467 , 112-116.
- Gaur, A., Varma, G. D. (2006). Magnetoresistance Behavior of $\text{La}_{0.7}\text{Sr}_{0.3}\text{MnO}_3/\text{NiO}$ Composites. *Solid State Communications* 139 , 310-314.
- Gross, G. M., Razavi, F. S., Habermeier, H.-U. (2000). Effect of Strain on the Properties of $\text{La}_{0.67}\text{Ca}_{0.33}\text{MnO}_3$. *Journal of Magnetism and Magnetic Materials* 211 , 41-46.

- Harzheim, G., Schubert, J., Beckers, L., Zander, W., Meertens, D., Osthover, C., Buchal, Ch. (1998). Colossal Magnetoresistance of thin films of $\text{La}_{0.66}\text{Ba}_{0.33}\text{MnO}_3$ as a Function of Film Thickness. *Materials Science and Engineering B56* , 147-151.
- Hsu, J. H., Hung, S. H., Biswas, S., Sharma, P., Lin, J. G. (2007). Enhancement of Ordering Temperatures of $\text{La}_{0.67}\text{Ca}_{0.33}\text{MnO}_3$ Thin Films by Adding Ho Atoms. *Physica Status Solidi (b)244* , 12.
- Hwang, H. Y., Cheong,, S.-H., Ong, N. P. and Batlogg, B. (1996). Spin-Polarized Intergrain tunneling in $\text{La}_{2/3}\text{Sr}_{1/3}\text{MnO}_3$. *Physical Review Letters 77(10)*: 2041-2044.
- Jeong, D., Joonghoe, D. (2010). Strain Effects on the Electric and Magnetic Properties of the Magnetoresistive $\text{La}_{0.7}\text{Ba}_{0.3}\text{MnO}_3$ Films. *IEEE Transactions on Magnetics 46* , 1883-1885.
- Kameli, P., Salamat, H., Aezami, A. (2008). Influence of Grain Size on Magnetic and Transport Properties of Polycrystalline $\text{La}_{0.8}\text{Sr}_{0.2}\text{MnO}_3$ Manganites. *Journal of Alloys and Compounds 450* , 7-11.
- Karishna, D. C., Venugopal Reddy, P. (2009). Magnetic Transport Behavior of Nanocrystalline $\text{Pr}_{0.67}\text{A}_{0.33}\text{MnO}_3$ (A=Ca, Sr, Pb and Ba) Manganites. *Journal of Alloys and Compounds 479* , 661-669.
- Krebs, H-U., Weisheit, M., Faupel, Jorg., Suske, E., Scharf, T., Fuhse, C., Stormer, M., Sturm, K., Seibt, M., Kijewski, H. (2003). Pulsed Laser Deposition (PLD) A Versatile Thin Film Technique. *Advances in Solid State Physics 43*,505-518.
- Knizek, K., Jirak, Z., Pollert, E., Zounova, F. (1992). Structure and Magnetic Properties of $\text{Pr}_{1-x}\text{Sr}_x\text{MnO}_3$ Perovskites. *Journal of Solid State Chemistry 100* , 292-300.
- Lei, L. W., Fu, Z. Y., Zhang, J. Y., Wang, H. (2006). Synthesis and Low Field Transport Properties in a ZnO -doped $\text{La}_{0.67}\text{Ca}_{0.33}\text{MnO}_3$ Composite. *Materials Science and Engineering B 128* , 70-74.
- Maignan, A., Varadaraju, U. V., Millange, F., Raveau, B. (1997). AC susceptibilities and size effect in $\text{Ln}_{0.7}(\text{Sr, Ca})_{0.3}\text{MnO}_3$. *Journal of Magnetism and Magnetic Materials , L237-L242*.
- Malisa, A., Ivanov, Z. (2005). Colossal Magnetoresistance Effect in Epitaxially Grown $\text{La}_{2/3}\text{Ca}_{1/3}\text{MnO}_3$ Perovskite-like Manganite Thin Films. *Journal of Magnetism and Magnetic Materials 295* , 277-283.
- Millis, A. J., Littlewood, P. B., Shraiman, B. I. (1995). Double Exchange Alone Does Not Explain the Resistivity of $\text{La}_{1-x}\text{Sr}_x\text{MnO}_3$. *Physical Review Letters 74 (25)* , 5144-5147.

- Miyazaki, T. (2004). *Spintronics: Fundamentals for Next Generation Memory MRAM*. Japan: Nikkan Kougyou Shinbun-sha.
- Pan, K. Y., Halim, S. A., Lim, K. P., Daud, W. M., Chen, S. K. (2011). Effect of Sintering Temperature on Microstructure, Electrical and Magnetic Properties of $\text{La}_{0.8}\text{K}_{0.15}\text{MnO}_3$ Prepared by Sol-Gel Method. *Journal of Superconductivity and Novel Magnetism*, DOI 10.1007/s10948-011-1392-1.
- Panwar, N., Sen, Vikram., Pandya, D. K., Agarwal, S. K. (2007). Grain Boundary Effects on the Electrical and Magnetic Properties of $\text{Pr}_{2/3}\text{Ba}_{1/3}\text{MnO}_3$ and $\text{La}_{2/3}\text{Ca}_{1/3}\text{MnO}_3$ Manganites. *Materials Letters* 61 , 4879-4883.
- Paranjape, M., Raychaudhuri, A. K. (2002). Annealing Induced Grain Growth and Grain Connectivity in an Epitaxial Film of $\text{La}_{0.67}\text{Ca}_{0.33}\text{MnO}_3$ and it's Effect on Low Field Colossal Magnetoresistance. *Solid State Communications* 123, 521-525.
- Paranjape, M., Raychaudhuri, A. K., Mathur, N. D., Blamire, M. G. (2003). Effect of Strain on the Electrical Conduction in Epitaxial Films of $\text{La}_{0.7}\text{Ca}_{0.3}\text{MnO}_3$. *Physical Review B (Condensed Matter and Materials Physics)* 67 , 214415.
- Park, S. Y., Lee, Y. P., Prokhorov, V. G. (2004). Effects of Lattice-Strain-Induced Distortion and Jahn-Teller Coupling in $\text{La}_{0.8}\text{Sr}_{0.2}\text{MnO}_3/\text{La}_{0.8}\text{Ca}_{0.2}\text{MnO}_3$ Epitaxial Films. *Journal of the Korean Physical Society* 45 (1) , 47-50.
- Praus, R. B., Gross, G. M., Razavi, F. S., Habermeier, H. -U. (2000). Effects of Strain on the Properties of $\text{La}_{0.67}\text{Ca}_{0.33}\text{MnO}_3$ Thin Films. *Journal of Magnetism and Magnetic Materials* 211, 41-46.
- Prasad, R., Singh, M. P., Siwach, P. K., Kaur, A., Fournier, P., Singh, H. K. (2010). Effect of Thickness on Magnetic Phase Coexistence and Electrical Transport in $\text{Nd}_{0.51}\text{Sr}_{0.49}\text{MnO}_3$ Films. *Applied Physics A* 99 , 823-829.
- Priolkara, K. R., Rawat, R. (2008). Effect of Heterovalent Substitution at Mn site on the Magnetic and Transport Properties of $\text{La}_{0.67}\text{Sr}_{0.33}\text{MnO}_3$. *Journal of Magnetism and Magnetic Materials* 320 , 325-330.
- Prokhorov, V. G., Komashko, V. A., Kaminsky, G. G. (2007). Magnetic and Transport Properties Driven by Lattice Strain in $\text{La}_{0.7}\text{Ca}_{0.3}\text{MnO}_3/\text{BaTiO}_3$ and $\text{La}_{0.7}\text{Sr}_{0.3}\text{MnO}_3/\text{BaTiO}_3$ Bilayer Films. *Low Temperature Physics* 33 (1) , 58-65.
- Ramirez, A. P. (1997). Colossal Magnetoresistance. *Journal of Physics: Condensed Matter* , 8171-8199.
- Raveau, B., Martin, C., Maignan, A., Hervieu, H. (2002). Insulator-Metal Like Transition in Air-synthesized Mn^{4+} Rich $\text{La}_{1-x}\text{BaMnO}_3$: Grain Boundary Phase Effect. *Journal of Physics: Condensed Matter* 14 , 1297.

- Raveau, R., Martin, C., Maignan, A. (1998). What About the Role of B Elements in the CMR Properties of ABO_3 Perovskites? *Journal of Alloys and Compounds* 275-277 , 461-467.
- Rodriguez-Martinez, L. M. and Attfield, J. P. (1996). Cation Disorder and Size Effects in Magnetoresistive Manganese Oxide Perovskites. *Physical Review B* 54 (22) , R15622-R15625.
- Rodriguez-Martinez, L. M., Attfield, J. P. (1998). Cation Disorder and the Metal-insulator Transition Temperatuer in Manganese Oxide Perovskites. *Physical Review B* 58 , 2426.
- Seman, T. F., Ahn, K. H. (2012). Effects of Rare-Earth Ion Size on The Stability of the Coherent Jahn-Teller Distortions in Undoped Perovskite Manganites. *Physical Review B* 86, 184106.
- Park, S. Y., Lee, Y. P. (2004). Effects of Lattice-Strain-Induced Distortion and Jahn Teller Coupling in $\text{La}_{0.8}\text{Sr}_{0.2}\text{MnO}_3/\text{La}_{0.8}\text{Ca}_{0.2}\text{MnO}_3$ Epitaxial Films. *Journal of the Korean Physical Society* 45 (1) , 47-50.
- Sahu, D. R., Roul, B. K., Pramanik, P., Jow- Lay Huang. (2005). Synthesis of $\text{La}_{0.7}\text{Sr}_{0.3}\text{MnO}_3$ Materials by Versatile Chemical Technique. *Physica B* 369 , 209-214.
- Shankar, S. K., Kar, S., Subbanna, G. N., Raychaudhuri, A. K. (2004). Enhanced Ferromagnetic Transition Temperature in Nanocrystalline Lanthanum Calcium Manganese Oxide ($\text{La}_{0.67}\text{Ca}_{0.33}\text{MnO}_3$). *Solid State Communications* 129,479-483.
- Taran, S., Karmakar, S., Chou, H., Chaudhuri, B. K. (2006). Transport Properties of Some Rare-earth Mono and Bilayer Manganite Films. *Physica Status Solidi (b)* 243 (8) , 1853-1861.
- Topsoe, H. (1968). *Geometric Factor in Four Point Resistivity Measurement.*
- Troyanchuk, I. O., Kolesova, I. M., Szymczak, H., Nabialek, A. (1997). Preparation, Magnetic and Transport Properties of $\text{A}_{0.66}\text{Ba}_{0.34}\text{MnO}_3$ (A=Pr, Nd, Sm, Eu, Gd) Perovskites. *Journal of Magnetism and Magnetic Materials* 176 , 267-271.
- Urushibara, A., Moritomo, Y., Arima, T., Kido, G., Tokura, Y. (1995). Insulator-Metal Transition and Giant Magnetoresistance in $\text{La}_{1-x}\text{Sr}_x\text{MnO}_3$. *Physical Review (b)* 51 , 14103-14109.
- Vengalis, B., Maneikis, A., Anisimovas, F., Butkute, R., Dapkus, L., Kindurys, A. (2000). Effect of Strains on Electrical and Optical Properties of Thin $\text{La}_{0.67}\text{Ca}_{0.33}\text{MnO}_3$ Films. *Journal of Magnetism and Magnetic Materials* 211 , 35- 40.

- Venkataiah, G., Prasad, V., Venugopal Reddy, P. (2007). Influence of A-site Cation Mismatch on Structural, Magnetic and Electrical Properties of Lanthanum Manganites. *Journal of Alloys and Compounds* 429 , 1-9.
- Wang, Z. M., Sang, G. Ni, H., Du, Y. W. (2001). The Effect of Average A-site Cation Radius on T_c in Perovskite Manganites. *Journal of Magnetism and Magnetic Materials* 234, 213-217.
- Yeh, N-C., Vasquez, R. P., Beam, D. A., Fu, C-C., Huynh, J., Beach, G. (1997). Effects of lattice distortion and Jahn-Teller Coupling on the Magnetoresistance of $\text{La}_{0.7}\text{Ca}_{0.3}\text{MnO}_3$ and $\text{La}_{0.5}\text{Ca}_{0.5}\text{CoO}_3$ Epitaxial Films. *Journal of Condens Matter* 9, 3713-3721.
- Zener, C. (1951). Interaction Between the d Shells in the Transition Metals. *Physical Review* 81(4) , 403-405.
- Zener, C. (1951). Interaction Between the d Shells in the Transition Metals, II. Ferromagnetic Compounds of Manganese with Perovskite Structure. *Physical Review* 82(3) , 403-405.
- Zhang, N., Ding, W., Xing, D. and Du, Y (1997). Tunnel-type giant magnetoresistance in the granular perovskite $\text{La}_{0.85}\text{Sr}_{0.15}\text{MnO}_3$. *Physical Review B* 56 (13): 8138-8142.
- Zhou, J. P., Mcdevitt, J. T., Zhou, J. S., Yin, H. Q., Goodenough, J. B. (1999). Effect of Tolerance Factor and Local Distortion on Magnetic Properties of the Perovskite Manganites. *Applied Physics Letters* 75 (8) , 1146.